JOURNAL OF Materials CHEMISTRY

An *in-situ* modified sol–gel process for monolith catalyst preparation used in the partial oxidation of methane

Ran Ran, Guoxing Xiong* and Weishen Yang

State Key Laboratory of Catalysis, Dalian Institute of Chemical Physics, Chinese Academy of Sciences, P.O. Box 110, Dalian 116023, China. E-mail: gxxiong@dicp.ac.cn

Received 26th November 2001, Accepted 12th February 2002
First published as an Advance Article on the web 15th April 2002

An *in-situ* modified sol–gel method for the preparation of a Ni-based monolith-supported catalyst is reported. With the presence of a proper amount of plasticizer and binder, and at an optimized pH value, the stable boehmite sol was modified with metal ions (Ni, Li, La) successfully without distinct growth of the particle size. Monolith-supported Ni-based/γ-Al_2O_3 catalysts were obtained using the modified sol as the coating medium with several cycles of dip-coating and calcination. Combined BET, SEM–EDS, XRD and H_2-TPR investigations demonstrated that the derived monolith catalysts had a high specific surface area, a relatively homogeneous surface composition, and a high extent of interaction between the active component and the support. These catalysts showed relatively stable catalytic activities for partial oxidation of methane (POM) to syngas under atmospheric pressure. The monolith catalysts prepared by this sol–gel method also demonstrated an improved resistance to sintering and loss of the active component during the reaction process.

1 Introduction

Catalytic conversion of methane through partial oxidation processes (POM: $CH_4 + 1/2\,O_2 \rightarrow CO + 2\,H_2$, $\Delta H_{298\ K} = -36$ kJ mol^{-1}) has drawn considerable attention recently.[1,2] In comparison with the traditional steam reforming process ($CH_4 + H_2O \rightarrow CO + 3\,H_2$, $\Delta H_{298\ K} = 206$ kJ mol^{-1}), partial oxidation possesses several advantages, including a higher space velocity operation, reduced capital and operation costs, an optimized $H_2:CO$ ratio, and so on. Among the many kinds of POM catalysts, Ni-based catalysts usually have excellent conversion and selectivity – almost the same as that of precious metal catalysts. Moreover, monolith-supported catalysts are currently of great interest for application in the POM reaction.[3–5] Among the different types of monoliths, foam monolith has a relatively high surface to volume ratio compared to commercial pellets, exhibits lower pressure drops during the reaction process, has a low thermal expansion coefficient, and good resistance to thermal shock.[5] Those properties make the foam monolith-supported catalysts extremely suitable for catalytic processes such as POM at high temperatures and high space velocity. Monolith-supported Ni-based catalysts have recently been investigated by some researchers for the POM reaction. Although the foam monolith is somewhat porous and rough-textured, it nonetheless has a relatively low surface area with respect to catalyst support requirements. Accordingly, it is usually deposited with a layer of washcoat such as γ-Al_2O_3 which serves as a support upon which finely dispersed catalytic metal may be deposited.[5]

Monolith-supported catalysts can be prepared *via* organometallic deposition, impregnation, or direct washcoating with the catalyst slurry. However, by these methods, it is usually difficult to deposit the catalyst components on the monolith surface as a homogeneous layer, and the interaction between active components and the support is not strong enough. Furthermore, during the subsequent calcination and reaction processes, the active components tend to aggregate, causing sintering, and lead to a decrease of the catalytic activity.[6] For example, some investigators have reported aggregation of the active metal after only several hours of calcination.[7] For an impregnated monolith-supported Ni-based catalyst, Schmidt and coworkers[8] have observed that the catalyst deactivated slowly during the reaction processes, methane conversion and hydrogen selectivity decreased by about 2%, larger metal particles formed and less than 0.1 wt% Ni remained on the front part of the catalyst after only 22 hours of POM operation. With a Ni-based monolith catalyst, Heitnes *et al.*[9] observed that the dispersion of nickel in a monolith catalyst decreased by 57% after only 7 hours of reaction at 800 °C. Others[10] have also reported similar unstable activity of the Ni monolith catalyst.

Consequently, in order to increase the activity and stability of monolith catalysts, it is critical to increase the thermal stability of the active metal (*i.e.* to diminish the sintering and evaporation of the active component), and to improve the interaction of the catalyst layer and substrate (for lowering physical losses of the active component). In this paper, we report on a modified sol–gel method to deposit a uniform thin layer of Ni-based/γ-Al_2O_3 catalysts over a monolith. The sol–gel method is well developed for the preparation of supported catalysts since it is 'easy to control', which can be described as the following advantages: the ability to maintain high purity, to control compositional homogeneity at a molecular level, and to introduce several components in a single step.[11–14] Moreover, the stronger metal–support interaction of the catalysts prepared by the sol–gel method provided good resistance to the loss and sintering of the active metal.[15] It is also merited for allowing the coating of thin films over different geometrical substrates,[16,17] and easily controllability of the layer thickness (*i.e.* the amount of catalysts) *via* changes in the dipping time and viscosity of the sol.[18] Considering the above-mentioned advantages, the sol–gel method should overcome the disadvantages of other monolith catalyst preparation methods. The preparation of monolith-supported catalysts *via* the sol–gel method can be carried out first by deposition of a high surface area porous layer on the monolith and then by impregnating the coated monolith with the catalytic components. With such a procedure, the benefit of the sol–gel method is only demonstrated by better control of the uniformity of the support layer and an improved strength between the monolith and the catalytic layer. In this study, we have developed a method for

 DOI: 10.1039/b110820b

the *in-situ* modification of a boehmite sol with Ni and other metal additives for the preparation of monolith-supported catalysts. Using such a procedure, the γ-Al_2O_3 support and the supported catalytic layer are both sol–gel derived, and thus the benefits of sol–gel preparation are embodied in both steps. As a result, the novel sol–gel derived monolith catalyst demonstrated relatively good metal dispersion and good catalytic stability in the POM process.

2 Experimental

2.1 Preparation

2.1.1 Modified sol–gel catalysts and monolith catalysts. PURAL SB powders (a mixture of boehmite and pseudo-boehmite powder, supplied by Condea, Germany) were used in the preparation of the boehmite sol. PEG [poly(ethylene glycol)] and PVA [poly(vinyl alcohol)] were supplied by Merck GmbH (Germany). Foam monoliths [supplied by Hi-Tech Ceramics, composed mainly of α-Al_2O_3 with small quantity of SiO_2, 45 pores per inch (ppi)] were cylindrically shaped with a diameter of 7 mm and a length of 10 mm before dip-coating. Other chemicals used in the preparation procedure were of AR Grade, supplied by the Shanghai Chemical Reagent Corporation.

The powders were hydrated with deionized water at 80 °C for 30–60 min, then peptized with 1.6 mol l^{-1} nitric acid.[19] The peptized sol was aged for 6–24 h at 80 °C to obtain a stable 1 mol l^{-1} boehmite sol (pH 3–4). Then, stoichiometric mixtures of nickel(II) nitrate (98%), lithium(I) nitrate (97%) and lanthanum(III) nitrate (La_2O_3 >44%) solutions were slowly added dropwise to the 1 mol l^{-1} boehmite sol with stirring for about 180 min to obtain a modified boehmite sol. The concentrations of the solutions were Ni^{2+} *ca.* 0.08 mol l^{-1} (corresponding to a Ni loading of 8.7 wt%), La^{3+} *ca.* 0.01 mol l^{-1} and Li^{+} *ca.* 0.01 mol l^{-1}. In the modified sol, the concentrations of boehmite sol and Ni^{2+} were *ca.* 0.5 mol l^{-1} and 0.04 mol l^{-1} respectively. The change in pH value of the final modified sol with the fresh sol was kept within 0.2, then 2–4% PVA [10 wt% poly(vinyl alcohol) solution] as binder and 1–2% PEG as plasticizer were added to adjust the viscosity of the sol, stirring for 90–180 min until it became stable and homogeneous again. The modified sol could then be used for the preparation of the catalysts supported on the monolith (referred to as the 'monolith catalyst') or the sol–gel derived catalysts (referred to as the 'sol–gel catalyst').

As to the preparation of the monolith catalysts, monoliths were first washed with water and ethanol in an ultrasonic bath then calcined in air at 850 °C for 180 min. The treated monoliths were dipped into the stable modified sol for 1–10 min till a sol layer was deposited, then dried in air at 5 °C to get rid of water slowly (for *ca.* 36–60 h) and calcined at 550 °C for 4 h. The above dip-coating and calcination processes could be repeated several times until enough catalyst was coated on the monolith. The coated monoliths, which were calcined at 850 or 950 °C for 4–9 h, were used in the catalytic reactions. The whole preparation process is shown in Fig. 1. As to the preparation of sol–gel catalysts, the modified sol was dried and calcined under the same conditions as with the monolith catalysts.

2.1.2 Impregnated catalyst. The impregnation catalyst (which is not supported on the monolith) was prepared by impregnating appropriate amounts of mixtures of nickel(II) nitrate, lithium(I) nitrate and lanthanum(III) nitrate solutions on a commercial γ-Al_2O_3 support for 24 h, then drying in air at 120 °C for *ca.* 12 h, calcining in air at 850 or 950 °C for 4–9 h. The loading of metals is similar to that of the monolith and sol–gel catalysts.

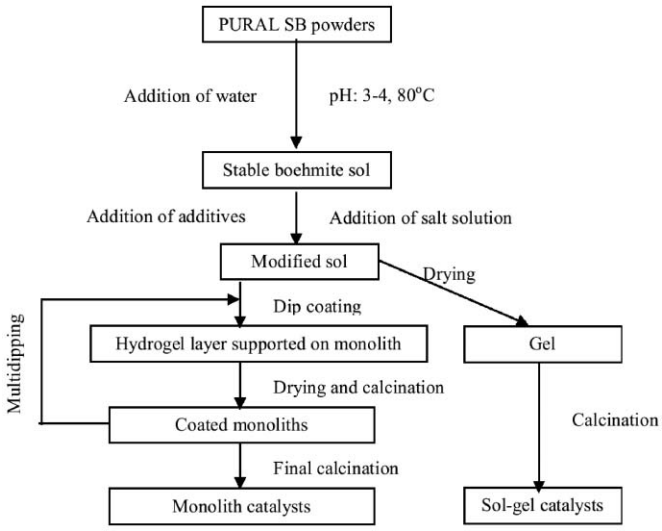

Fig. 1 Schematic representation of catalyst preparation by the modified sol–gel method.

2.2 Catalytic reaction

The POM reaction was carried out in a fixed-bed quartz reactor. The annular space between the monolith catalyst and the quartz tube was sealed with a high temperature alumina–silica-cloth to minimize bypass of the reactant gases around this space. In general, 20 mg (monolith weight is not included) of catalyst were used for the reaction. The GHSV was calculated using the weight of the catalyst layer. A thermocouple was placed at the exit of the catalyst to facilitate control of the electric furnace temperature. The reaction was performed at atmospheric pressure, 850 °C, with a space velocity of 13.4 × 10^4 l kg^{-1} h^{-1}. CH_4 (99.95% purity) and O_2 (99.99% purity) were fed into the reactor in the ratio of 2.0 : 1.0. Catalysts were not induced through any methods before reaction.

Product gases were analyzed using an on-line HP4890 GC equipped with a TDX-01 column using a TCD detector, and helium as the GC carrier gas. Water was condensed before the tail gas was analyzed. Standard gases were used to calibrate the concentrations of product gases (H_2, CO, CH_4, CO_2).

2.3 Characterizations of catalysts

XRD characterization was performed with a Riguku D/Max-RB X-ray diffractometer using a copper target at 40 kV × 100 mA at room temperature and a scanning speed of 8° min^{-1}. The different phases were identified using the JCPDS Powder Diffraction Files.[20] The crystal sizes were estimated according to X-ray diffraction using the Scherrer equation $D = k\lambda/B\cos\theta$.

The temperature-programmed reaction (TPR) experiment was performed as follows. The catalysts were placed into a quartz reactor (i.d. 4 mm), which was immersed in an electronically controlled furnace. The oven was heated at a rate of 10 °C min^{-1} from 50 to 1050 °C. Meanwhile, a 5% H_2–Ar mixture gas swept the catalyst at a constant flow rate of 30 ml min^{-1}. Hydrogen consumption was determined using an *in-situ* thermal conductivity detector (TCD) with a computer data acquisition system.

Surface areas of the catalysts were obtained from the nitrogen adsorption and desorption isotherm at 77 K using a Brunauer–Emmet–Teller (BET) surface analyzer (Coulter 100CX, USA). Before recording the isotherms, samples (*ca.* 50 mg) were previously desorbed at 300 °C under vacuum (10^{-6} Torr) for 2 h.

Thermogravimetric analysis (TGA) was performed with a Perkin-Elmer TGS-2. Air was used as the treated gas at a flow rate of 30 ml min^{-1} from room temperature to 1000 °C. The

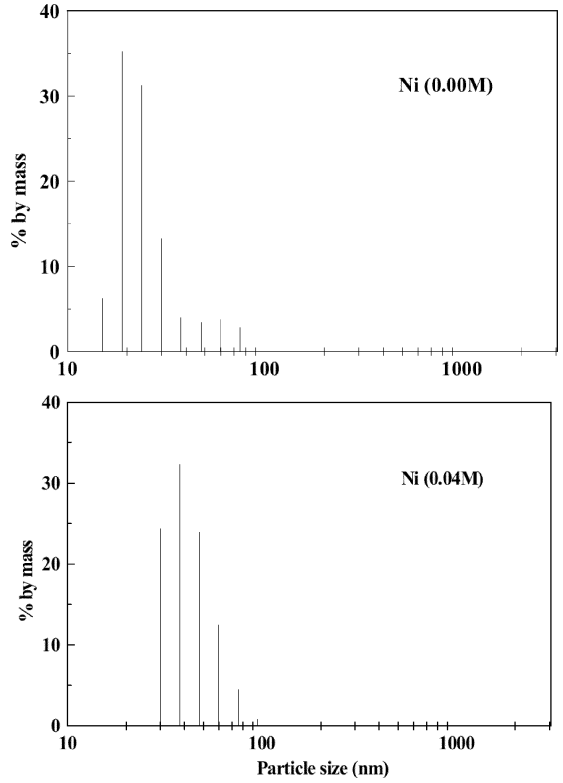

Fig. 2 Particle size distribution of the fresh sol (Ni 0.00 M) and the modified sol (Ni 0.04 M).

heating rate was 10 °C min^{-1}. Before testing, samples (20 mg) were dried at 120 °C for about 60 min.

Morphologies and elemental surface composition of fresh and used catalyst layers (supported over monoliths) were examined by scanning electron microscopy (SEM) (JEM-5600LV) with energy dispersive spectroscopy (EDS) (Oxford ISIS-300). After the POM reaction, the used catalyst was re-oxidized in air, and then it was used in the SEM–EDS analyses.

Particle sizes for the fresh and modified sols were determined using a Coulter N4 Plus Particle Sizer Analysizer, using photon correlation spectroscopy for measuring sol particle diameters in the range of 3–3000 nm. A He–Ne laser operating at 10 mW was used as the light source.

3 Results and discussion

3.1 Catalyst preparation

The particle size distributions of the fresh and modified sols are shown in Fig. 2. The particle size of the boehmite sol was almost totally located between 10 and 100 nm, with more than 80% in the narrow range of 20–30 nm. As for the modified sol, the particle size increased somewhat; and was mainly in the range of 30–100 nm (>99%), with most particles (>80%) being in the 30–50 nm range. The increase in particle size for the modified sol was caused by ion addition. The positive charge of the metal ions could destroy the double layer structure (which prohibits the sol from aggregation) such that some of the particles congregated to form larger particles until a new

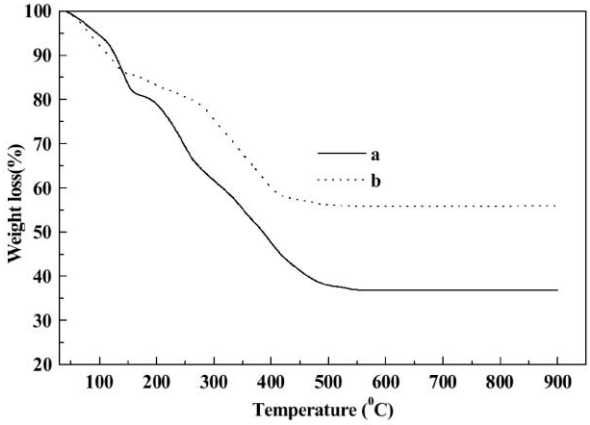

Fig. 3 Thermal analysis of sol–gel catalysts: (a), sol–gel catalyst with organic additives, (b) sol–gel catalyst without organic additives.

balance was established. However, comparing the particle size distributions of fresh and modified sols, we can notice that the increase in particle size after the addition of metal ions was not serious. No large particles (>3000 nm) was observed in the modified sol, and remained as a mono-distribution. It seems that the addition of metal ions did not destroy the homogeneous character of the boehmite sol remarkably. This can be explained as follows: (1) the pH value of the sol increased only by *ca.* 0.16 after the modification by metal ions, which was still within the pH value range of the stable sol; (2) the low concentration of metal ions could not destroy the stability of the sol completely. The above results demonstrated that by controlling the modification conditions carefully, it was feasible to modify *in-situ* the boehmite sol for dip-coating without reducing the homogeneity of catalyst to any great extent.

It is believed that the introduction of a plasticizer and binder into the sol is necessary to improve the coating quality.[21] A suitable amount of additives would not lead to significant changes in the microstructure of the coated layer.[21] However, catalysts must be calcined at a temperature higher than the lowest temperature needed to totally burn out the organic additives. The calcination temperature was determined by TGA. Fig. 3 shows the TGA profiles of the catalysts. No weight loss events can be detected when the calcination temperature is higher than *ca.* 550 °C, indicating that all of the organic compounds have been burnt out. Therefore, temperatures higher than 550 °C were selected for calcination. The catalyst amount loaded on to the monolith after each dip-coating is shown in Table 1. The loading amount for each dip-coating was almost the same, independent of how many times the dip-coating had been performed previously. However, when the amount of the additive was increased, the weight of the coated catalyst for each dip-coating increased clearly. It indicated that additives could greatly influence the catalyst layer thickness on the substrate as is reported in the literature.[21] Whereas the increase in additive amount could increase the loading amount of catalyst per dip-coating procedure, it could also influence the microstructure of the supported catalyst such that the amount of additive was critical. In this study we chose the additive amount to be in the range of 1–4%.

After the final calcination, a thin layer of catalyst was coated uniformly on the surface of monolith, as shown in Fig. 4. The

Table 1 Catalyst weight changes on the monolith after dip-coating

	W_1/mg	W_2/mg	W_3/mg	W_4/mg	W_5/mg
Catalyst weight/mg	4.0	8.6	13.4	17.3	19.4
	$W_1 - W_0$[b]	$W_2 - W_1$[c]	$W_3 - W_2$[c]	$W_4 - W_3$[b]	$W_5 - W_4$[a]
ΔW/mg	4.0	4.6	4.8	3.9	2.1

[a]PVA, 1%; PEG, 0.5%. [b]PVA, 2%; PEG, 1%. [c]PVA, 4%; PEG, 2%.

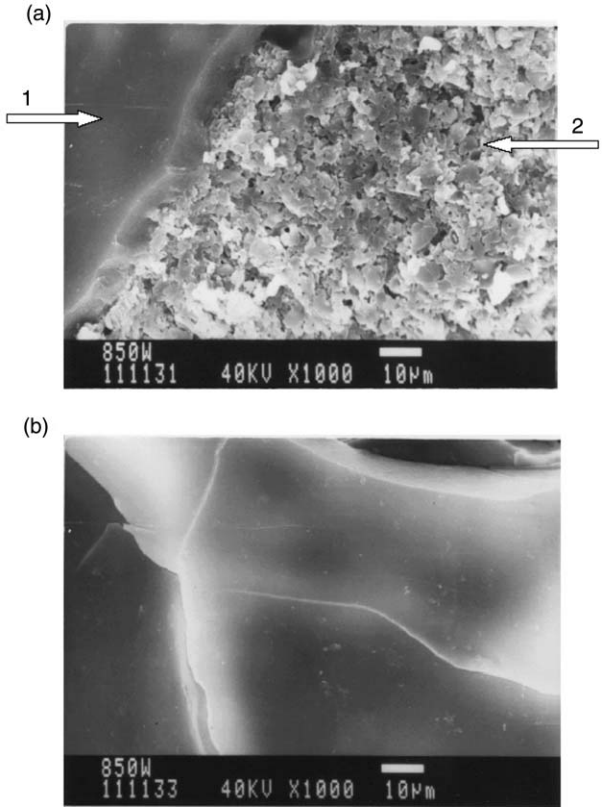

Fig. 4 Micrographs of monolith catalysts calcined at 850 °C. (a) Surface of monolith and catalyst layer (× 1000): arrow 1, layer of catalyst; arrow 2, typical surface of foam monolith. (b) Surface of catalytic layer (× 1000).

arrow 2 of Fig. 4(a) indicates the typical foam monolith surface, and arrow 1 points to the catalytic layer. The catalyst almost completely covered the surface of the monolith and was very uniform [Fig. 4(b)]. After several cycles of dip-coating and calcination, the thickness of catalytic layer was *ca.* 10 μm. As shown in Fig. 4(a), the catalyst layer joined with the monolith strongly, and no breakaway of the catalyst from the monolith support was observed. From Fig. 4(b) we find that, after calcination, no large polycrystallites appeared, which have been found on monolith catalysts prepared *via* another method.[22] The specific surface areas of the different catalysts are listed in Table 2. The catalysts prepared by the sol–gel method demonstrated larger surface areas than those of the catalyst prepared through the impregnation method. The higher surface area implies a higher dispersity of the active metal.

X-Ray diffraction patterns of the catalysts calcined at different temperatures are given in Fig. 5. The diffraction peaks were very broad, indicating small crystallite sizes and low crystallinity. The crystallite size estimated from the XRD results was found to be smaller than 3 nm. A slight increase of crystallite size with increasing calcination temperature was observed according to the peak width and intensity. When the catalyst was calcined at 950 °C for 9 h, the diffraction peaks of $LaAlO_3$ appeared. However, no characteristic diffraction peak of NiO appeared under all calcination conditions, which

Table 2 Influence of calcination temperature on catalytic surface area

T/°C	Surface area of sol–gel catalyst/m^2 g^{-1}	Surface area of impregnation catalyst/m^2 g^{-1}
850	103.97	93.08
900	88.76	67.10
950	58.84	55.79

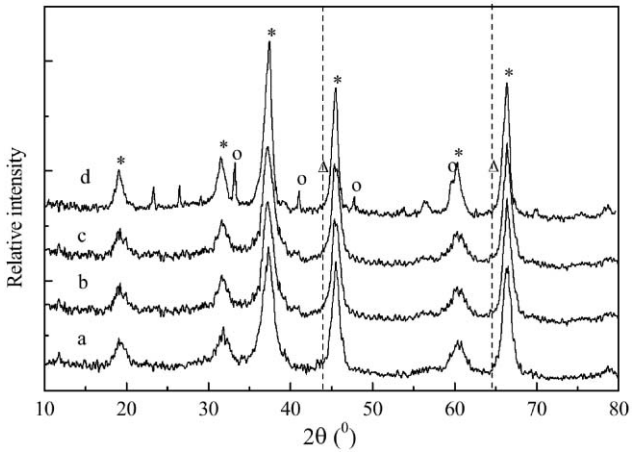

Fig. 5 X-Ray diffraction patterns of the catalysts: (a) impregnated catalyst calcined at 850 °C; (b–d) sol–gel derived catalysts: (b) calcined at 850 °C; (c) calcined at 900 °C; (d) calcined at 950 °C; with indicators: * $NiAl_2O_4$, ○ $LaAlO_3$, △ the position where the diffraction patterns of NiO should appear.

implies very small NiO crystallite sizes and a strong interaction between Ni and γ-Al_2O_3.

Fig. 6 shows the H_2-TPR profiles of the prepared catalysts calcined at different temperatures. Two reduction peaks appeared for the monolith catalyst calcined at 850 °C: the low-temperature reduction peak appeared at about 650 °C, and the other one appeared at about 850 °C. When the catalyst was calcined at 950 °C, the low-temperature reduction peak became much smaller, while the reduction peak of high temperature became broader and higher. Rynkowski *et al.*[23] and Dewaele and Froment[24] believed that the reduction peak at the higher temperature corresponded to the reduction of the crystal $NiAl_2O_4$ spinel, and the increase in crystallinity led to the increase in peak temperature. Rynkowski *et al.*[23] and Zhang *et al.*[25] further pointed out that the amorphous phase of Ni^{2+} species would be reduced in the temperature range of 575–660 °C, and that the spinel phase would be reduced above 690 °C with T_m values between 750 and 830 °C for the impregnated catalysts. Zhang *et al.*[25] believed that while the Ni^{2+} ions diffuse into the surface lattice of γ-Al_2O_3 during the dispersion, the Al^{3+} ions will counter-diffuse to the surface lattice of NiO crystallites to form the amorphous phase of Ni^{2+}, which becomes less reducible. Since all catalysts calcined at 850–950 °C were bright blue (the typical color of the $NiAl_2O_4$ spinel) and no possible free NiO was seen (the reduction peak for free

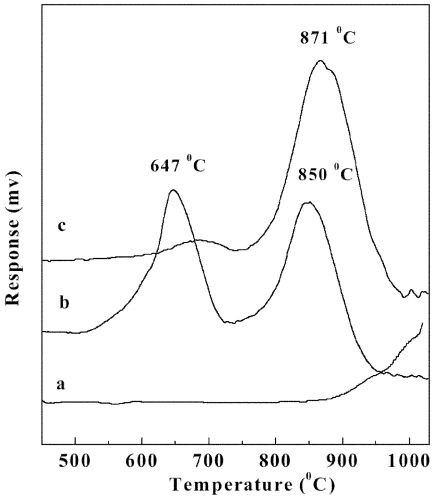

Fig. 6 H_2-TPR profiles of (a) bulk $NiAl_2O_4$, (b) monolith catalyst calcined at 850 °C, (c) monolith catalyst calcined at 950 °C.

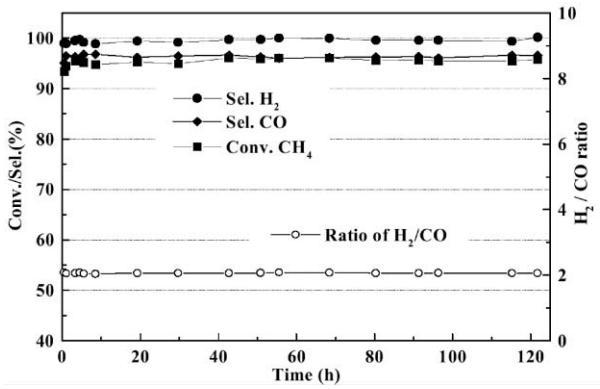

Fig. 7 Reaction performance of LiLaNiO/γ-Al_2O_3 monolith catalyst as a function of time ($CH_4:O_2 = 2.0$, GHSV $= 13.4 \times 10^4$ l kg^{-1} h^{-1}, $T = 850$ °C).

NiO should be around 400 °C), the first reduction peak in this study should correspond to the reduction of amorphous phase Ni^{2+}, and the second peak should correspond to reduction of the crystalline spinel. The increase in the calcination temperature led to the increase of crystallinity of the catalyst. According to the XRD and TPR results, a strong interaction between Ni and γ-Al_2O_3 formed as expected. Strong interaction of Ni with Al_2O_3 is believed to successfully prohibit the evaporation and aggregation of Ni during the operation.[26,27] The TPR profile of bulk $NiAl_2O_4$ is given for comparison with the monolith catalyst. It is much more difficult to be reduced than the monolith catalyst, which could be assumed as being the reason for the better crystallinity of bulk $NiAl_2O_4$ as Dewaele *et al.*[24] believed.

3.2 Evaluation of Ni-based catalysts supported on monoliths

The as-prepared monolith catalyst was used for the POM reaction. The catalytic stability is shown in Fig. 7. Under conditions of 850 °C, $CH_4:O_2 = 2.0$ and space velocity of 13.4×10^4 l kg^{-1} h^{-1}, the activity of the monolith catalyst remained very stable during an operation of *ca.* 120 h. No distinct deactivity appeared during the reaction. Methane conversion, selectivity of carbon monoxide and the yield of the carbon monoxide remained higher than 95, 96 and 92%, respectively.

In comparisons of the elemental surface composition (by EDS) of the front part of the fresh catalyst with the used catalyst, only about 7% Ni loss was detected after 120 h of the POM reaction. The small amount of nickel loss did not cause a change in catalyst activity. Additionally, no obvious black coke was found over the catalyst and the walls of the quartz reactor. From the examination of SEM–EDS, no obvious carbon deposition was detected on the used monolith catalyst. Fig. 8 shows the microstructure of the catalytic layer after *ca.* 120 h of the POM reaction. The surface of catalytic layer did not change significantly: it looked uniform, like the fresh catalyst, which proved that sintering did not happen. However, some crevices appeared after the reaction, but that was less likely to be due to the sintering of the active metal since sintering should lead to large connected particles with rounded features.[7] The expansion coefficients are somewhat different for the catalytic layer and monolith, and hence crevices are formed during the oxidation and reduction reactions at such a high reaction temperature. Too many crevices would cause flaking away of the catalytic layer, and result in shortening of the usage time of the monolith catalyst. A study on optimization of the reduction of crevices during utilization is underway.

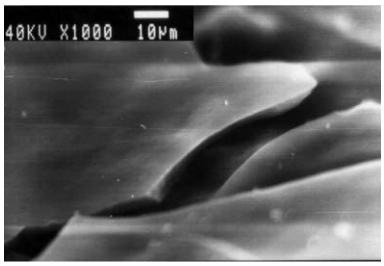

Fig. 8 Micrograph ($\times 1000$) of the monolith catalyst after 120 h of the POM reaction at 850 °C.

4 Conclusions

An *in-situ* modified sol–gel method has been used for the preparation of catalysts supported on monoliths for the reaction of the partial oxidation of methane to syngas. The boehmite sol was successfully modified with the active component without obvious growth of the particle size. Using the modified sol as the dip-coating medium, a thin layer of catalyst with a high surface area and high dispersion of the active component was coated uniformly on the surface of the monolith. The as-prepared monolith catalysts have a strong interaction between the catalyst and the support, as well as between the catalyst layer and the monolith, which helped to prohibit the sintering and loss of the active component.

The as-prepared catalyst demonstrated good performance for the POM reaction with high activity and operation stability. After *ca.* 120 h of operation of the POM reaction at high temperatures, the activity of the catalyst supported on the monolith remained stable, with methane conversion higher than 95% and CO selectivity higher than 96%. This demonstrated that the new sol–gel method is suitable for the preparation of monolith-supported catalysts, at least for Ni-based/γ-Al_2O_3. The catalyst can be operated for the partial oxidation of methane to syngas at a very high space velocity (13.5×10^4 l kg^{-1} h^{-1}) with a relatively stable activity.

Acknowledgements

This work was supported by the National Advanced Materials Committee of China (Grant No. 715-006-0122) and the Ministry of Science and Technology, China (Grant No. G1999022401).

References

1 A. T. Ashcroft, A. K. Cheetham, J. S. Foord, M. L. H. Green, C. P. Grey, A. J. Murrell and P. D. F. Vernon, *Nature*, 1990, **334**, 319.
2 Q. Miao, G. Xiong, S. Sheng, W. Cui, L. Xu and X. Guo, *Appl. Catal. A.*, 1997, **154**, 17.
3 J. K. Hochmuth, *Appl. Catal. B.*, 1992, **1**, 89.
4 K. H. Hofstad, O. A. Rokstad and A. Holmen, *React. Kinet. Catal. Lett.*, 1997, **60**, 357.
5 H. S. Hwang, R. M. Heck and R. M. Yarrington, *US Pat.*, No. 4,522,894, 1985.
6 E. Ruckenstein and H. Y. Wang, *J. Catal.*, 1999, **187**, 151.
7 D. A. Hickman, E. A. Haupfear and L. D. Schmidt, *Catal. Lett*, 1993, **17**, 223.
8 P. M. Torniainen, X. Chu and L. D. Schmidt, *J. Catal.*, 1994, **146**, 1.
9 K. Heitnes, S. Lindberg, O. A. Rokstad and A. Holmen, *Catal. Today*, 1994, **21**, 471.
10 M. G. Poirier, J. Trudel and D. Guay, *Catal. Lett.*, 1993, **21**, 99.
11 T. Ueckert, R. Lamber, N. I. Jaeger and U. Schubert, *Appl. Catal. A.*, 1997, **155**, 75.
12 B. Breitscheidel, J. Zieder and U. Schubert, *Chem. Mater.*, 1991, **3**, 559.
13 W. Zou and R. D. Gonzalez, *Appl. Catal. A.*, 1995, **126**, 351.
14 J. A. Montoya, E. Romero-Pascual, C. Gimon, P. Del Angel and A. Monzon, *Catal. Today*, 2000, **63**, 71.
15 Y. Zhang, G. Xiong, S. Sheng and W. Yang, *Catal. Today*, 2000, **63**, 517.
16 Y. Chen, X. Ai, C. Huang and B. Wang, *Mater. Sci. Eng. A*, 2000, **288**, 19.

17 Y. S. Lin, K. J. De Vries and A. J. Burggraaf, *J. Mater. Sci.*, 1991, **26**, 715.
18 R. S. A. De Lange, J. H. A. Hekkink, K. Keizer and A. J. Burggraaf, *J. Membrane Sci.*, 1995, **99**, 57.
19 A. W. Li, H. B. Zhao, J. H. Gu and G. X. Xiong, *Sci. China., Ser. B: Chem.*, 1997, **40**, 31.
20 JCPDS, Swarthmore, PA.
21 R. J. R. Uhlhorn, M. H. B. J. Huis in't Veld, K. Keizer and A. J. Burggraaf, *J. Mater. Sci.*, 1992, **27**, 527.
22 D. A. Hickman and L. D. Schmidt, *J. Catal.*, 1992, **138**, 267.
23 J. M. Rynkowski, T. Paryjczak and M. Lenik, *Appl. Catal. A.*, 1993, **106**, 73.
24 O. Dewaele and G. F. Froment, *J. Catal.*, 1999, **184**, 499.
25 L. Zhang, J. Lin and Y. Chen, *J. Chem. Soc., Faraday Trans.*, 1992, **88**, 497.
26 M. Montes, C. Penneman de Bosscheyde, B. K. Hodnett, F. Delannay, P. Grange and B. Delmon, *Appl. Catal.*, 1984, **12**, 309.
27 M. A. Keane and P. M. Patterson, *J. Chem. Soc., Faraday Trans.*, 1996, **92**, 1413.